Effect of three-body loss on itinerant ferromagnetism in an atomic Fermi gas

G. J. Conduit and E. Altman

Phys. Rev. A **83**, 043618 — Published 20 April 2011

DOI: 10.1103/PhysRevA.83.043618

Effect of three-body loss on itinerant ferromagnetism in an atomic Fermi gas

G.J. Conduit[1,2,*] and E. Altman[1]

[1] *Department of Condensed Matter Physics, Weizmann Institute of Science, Rehovot, 76100, Israel*
[2] *Physics Department, Ben Gurion University, Beer Sheva, 84105, Israel*

(Dated: March 2, 2011)

A recent experiment has provided the first tentative evidence for itinerant ferromagnetism in an ultracold atomic gas. However, the interpretation of the results is complicated by significant atom losses. We argue that during the loss process the system gradually heats up but remains in local equilibrium. To quantify the consequences of atom loss on the putative ferromagnetic transition we adopt an extended Hertz-Millis theory. The losses damp quantum fluctuations thus increasing the critical interaction strength needed to induce ferromagnetism, and revert the transition from being first to second order. This effect may resolve a discrepancy between the experiment and previous theoretical predictions. We further illuminate the impact of loss by studying the collective spin excitations in the ferromagnet. Even in the fully polarized state, where loss is completely suppressed, spin waves acquire a decay rate proportional to the three-body loss coefficient.

PACS numbers: 03.75.Ss, 71.10.Ca, 67.85.-d

I. INTRODUCTION

The Stoner transition from a paramagnetic metal to a ferromagnet is one of the earliest known and seemingly simple examples of a quantum phase transition. Yet recent theoretical work [1–5] has revealed a great deal of complexity and suggests that quantum fluctuations play a vital role in determining the behavior near to the quantum critical point. Specifically, fluctuations drive the ferromagnetic transition first order at low temperature and may lead to the formation of novel phases [2, 5]. Whether these effects can explain puzzling experimental observations in materials such as $ZrZn_2$ and $Sr_3Ru_2O_7$ [7], or if coupling to phonons or other auxiliary degrees of freedom is involved remains an open question. Ultracold Fermi gases tuned by a Feshbach resonance now offer a concrete platform from which to answer such questions [4] and enhance our understanding of quantum critical phenomena in itinerant ferromagnets [8, 9]. A recent experiment [10] has provided the first evidence that could be consistent with a ferromagnetic state [4, 6, 11, 12], but cannot definitively prove that some other strongly correlated phase [13] was not formed. A major obstacle to the identification of a ferromagnetic phase in an ultracold atomic gas is the loss of atoms due to three-body interactions [6, 10, 14].

In this paper we demonstrate how the consequences of loss extend far beyond a simple fall in atom number. We highlight the quantum effects of the loss, showing that they induce fundamental changes in the phase diagram. Motivation for such an analysis comes in part from studies of one-dimensional Bose gases, where it was shown that the mere potential for significant two-body loss can give rise, all by itself, to Tonks-Girardeau correlations in the gas [15]. In the itinerant fermion system, we discover that three-body losses damp quantum fluctuations, which are vital in the establishment of the equilibrium phase diagram [1, 2, 4, 5]. Consequently the phase transition reverts from first to second order. Moreover, the critical interaction strength required to stabilize the ferromagnetic state increases significantly, from $k_F a \approx 1.2$ in the equilibrium theories [6, 11] to $k_F a \approx 2.4$, thus resolving a discrepancy with the experimental signature at $k_F a \approx 2.2$. We further predict that spin-waves of the ferromagnetic phase acquire a finite lifetime in the presence of loss and propose a new experimental protocol to observe this effect.

Before proceeding let us outline the structure of the paper. In section II we derive an effective action for the Fermi gas in the repulsive branch of the resonance, taking into account the effect of loss. This is done by integrating both over molecules formed virtually in two-body collisions and over molecules and fast particles formed from three-body collisions. The latter give rise to an imaginary three-body term in the action, which we show generates imaginary single particle and two-body terms in the action upon renormalization to low energies. In section III we adapt the generalized RPA formalism, previously used to analyze the itinerant ferromagnetic transition [9], to include the new terms due to loss. The phase diagram, obtained from the Ginzburg-Landau free energy thus derived, is presented in section IV. In this section we also discuss the impact of loss on the collective spin excitations of the ferromagnet and propose experimental protocols to measure their dispersion and lifetime. In section VI we justify the effective-equilibrium approach used in the previous sections. By solving kinetic equations of the Fermi gas, we show that the combination of loss and relaxation gives rise to an effective equilibrium distribution with slowly varying temperature and chemical potential. For a wide parameter regime, the heating rate is sufficiently slow to be considered adiabatic with respect to the quantum corrections discussed in section III. We conclude in section VII with a summary and outlook.

II. RENORMALIZATION OF INTERACTIONS

Our goal is to calculate the quantum partition function with a fermionic coherent state path integral $\mathcal{Z} = \int \mathcal{D}(\psi,\bar{\psi}) \exp\left(-S[\psi,\bar{\psi}]\right)$. A common difficulty in addressing the Stoner transition is that it occurs at an intermediate coupling regime, with no small parameter to control a fluctuation expansion. The standard approach is to tackle the problem from the weak coupling or dilute limit, with the expectation, that at least qualitative features of the analysis persist near to the transition point [1–4, 9]. This expectation is indeed supported by Quantum Monte-Carlo studies of a lossless model [5, 16, 17]. Here we adopt the same strategy, assuming the dilute limit in deriving the effective interactions including the effects of loss. In particular, the dominant loss mechanism in the dilute limit is the so called three-body loss [6, 10, 14].

A common starting point for addressing the Stoner instability in ultracold atomic gases is the effective action for a two component Fermi gas with a repulsive contact interactions

$$S = \int_0^\beta \mathrm{d}\tau \mathrm{d}\mathbf{r} \left[\sum_\sigma \bar{\psi}_\sigma \left(\partial_\tau + \epsilon_{\mathbf{k}} - \mu\right) \psi_\sigma + g \bar{\psi}_\uparrow \bar{\psi}_\downarrow \psi_\downarrow \psi_\uparrow \right]. \quad (1)$$

Here $\beta = 1/k_{\mathrm{B}}T$ is the inverse temperature and we have also set $\hbar = m = 1$. The two component atoms are represented by the Grassman fields $\bar{\psi}, \psi$ and are characterized by the single particle dispersion $\epsilon_{\mathbf{k}} = k^2/2$. The interaction is represented here by a repulsive s-wave contact potential $g\delta^3(\mathbf{r})$. It is important to note however that the microscopic interaction is in fact attractive, and in the regime of interest it supports a two-body bound state (Feshbach molecule). This degree of freedom is missing in the action (1). The bound state has been integrated out to give the effective repulsive interaction, as the two body T-matrix for scattering at positive energies. In (1) the T-matrix is approximated by its zero energy limit which is energy independent, or in other words an effective contact interaction. This will have to be regularized properly to avoid ultra-violet divergences. It is also important to note, that since the bound molecular state has been integrated out to obtain (1), the effect of loss the effect of loss into the molecular state is not included in this formalism.

Let us now derive the effective action taking the atom loss into account. In the cold atom gas at low densities ($k_{\mathrm{F}}a \ll 1$, where k_{F} is the Fermi wave vector and a is the s-wave scattering length), the loss occurs following a three-body collision in which two atoms bind to a Feshbach molecule and the third atom removes the excess energy. To introduce the effect of loss into the effective action we have to integrate out the bound state, while including the three-body processes in addition to the two body T-matrix in Fig. 1(a). The appropriate Feynman diagrams for the 3-body T-matrix are shown in Fig. 1(b) and (c). The resulting contribution of 3-body interactions to the action is

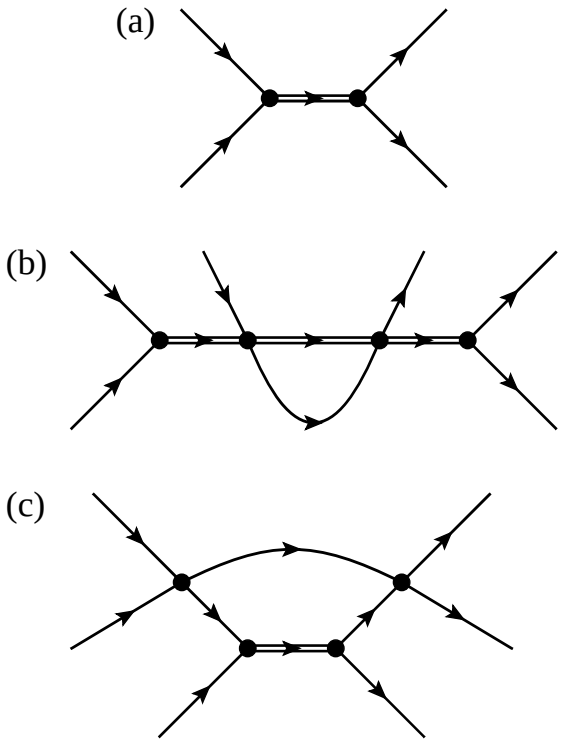

FIG. 1: (Color online) Three Feshbach molecule formation processes; (a) a second order process that can form only virtual unstable molecules, which can be stabilized by a third atom in processes (b) and (c). The single line corresponds to fermions, and double lines to Feshbach molecules.

$$\mathrm{i}\lambda' \int \mathrm{d}\mathbf{r}\mathrm{d}\mathbf{R} \bar{\psi}_\uparrow(\mathbf{R}+\mathbf{r}) \bar{\psi}_\downarrow(\mathbf{R}+\mathbf{r}) [\bar{\psi}_\uparrow(\mathbf{R}) \psi_\uparrow(\mathbf{R}) + \bar{\psi}_\downarrow(\mathbf{R}) \psi_\downarrow(\mathbf{R})] \times \psi_\downarrow(\mathbf{R}+\mathbf{r}) \psi_\uparrow(\mathbf{R}+\mathbf{r}) f(\mathbf{r}), \quad (2)$$

where λ' is real and $f(\mathbf{r})$ spans the range $\sim a$ over which the putative Feshbach molecule can interact with a third atom to carom its excess energy. We adopt the normalization for the Feshbach molecule potential of $\int \mathrm{d}\mathbf{r} f(\mathbf{r}) = 1$.

Note that we obtain an imaginary 3-body interaction. This is because both the bound state and the outgoing fast particle, which are integrated over, are on-shell and describe a physical decay process. That we obtained an imaginary term in the action should not come as a surprise, as it merely betrays the fact that the system is initialized in an unstable state and is therefore out of equilibrium. We shall nevertheless continue with the analysis of the effective action within the Matsubara formalism assuming that the system can be considered as being in quasi-equilibrium. Later, in Sec. VI we shall provide arguments which justify this hypothesis.

To further simplify the interaction we consider the dilute (weak interaction) limit $k_{\mathrm{F}}a \ll 1$. In this regime the molecule is small compared to the average particle separation and we can therefore make a gradient expansion in the fields of Eq. (2). It is also natural to turn to

a momentum space representation. Next, we note that single particle terms and two-body interactions are generated upon integrating out high energy Fermions perturbatively in λ

$$\frac{\mathrm{i}\lambda}{2}\Bigg[\bar{\rho}_\uparrow\bar{\rho}_\downarrow\sum_{\sigma,\mathbf{k}}k^2\bar{\psi}_{\sigma\mathbf{k}}\psi_{\sigma\mathbf{k}}+\frac{\bar{\rho}_\uparrow}{V}\sum_{\mathbf{k},\mathbf{k}',\mathbf{q}}\mathbf{k}\cdot\mathbf{k}'\bar{\psi}_{\uparrow\mathbf{k}}\bar{\psi}_{\downarrow\mathbf{k}'+\mathbf{q}}\psi_{\downarrow\mathbf{k}+\mathbf{q}}\psi_{\uparrow\mathbf{k}'}+\frac{\bar{\rho}_\downarrow}{V}\sum_{\mathbf{k},\mathbf{k}',\mathbf{q}}\mathbf{k}\cdot\mathbf{k}'\bar{\psi}_{\uparrow\mathbf{k}+\mathbf{q}}\bar{\psi}_{\downarrow\mathbf{k}'}\psi_{\downarrow\mathbf{k}}\psi_{\uparrow\mathbf{k}'+\mathbf{q}}\Bigg], \tag{3}$$

where $\bar{\rho}_\sigma$ is the average density of species σ, V is the system volume, and $\lambda = 3a^2\lambda'/10$. We shall retain only these terms in the action, which are much more relevant at low energies than the original original three-body interaction [18].

III. FERROMAGNETISM

We are now in a position to study the consequences of atom loss within the standard formalism established to treat fluctuations in itinerant ferromagnets [9], taking into account the effective interactions (3) generated by the three-body loss.

Before proceeding we generalize the formalism by introducing an atom source term of the form $-\mathrm{i}\gamma\sum_\sigma\bar{\psi}_\sigma\psi_\sigma$ into the action. For the most part we shall set $\gamma = 0$, which describes the physical system at hand. However there is conceptual appeal to consider a source with $\gamma > 0$ that can counterpoise the atom loss and thus lead to a true steady-state, in which the notion of a phase transition can be better defined. The source term also provides a template of how to apply the formalism to other physical systems such as polaritons in which laser pumping cancels particle loss. Within this formalism, the action is now

$$S=\int_0^\beta\mathrm{d}\tau\mathrm{d}\mathbf{k}\Bigg[\sum_\sigma\bar{\psi}_{\sigma\mathbf{k}}\left(\partial_\tau+\epsilon_\mathbf{k}+\mathrm{i}\lambda\bar{\rho}_\uparrow\bar{\rho}_\downarrow k^2-\mu-\mathrm{i}\gamma\right)\psi_{\sigma\mathbf{k}}+\int\mathrm{d}\mathbf{k}'\mathrm{d}\mathbf{q}\left[g+\mathrm{i}\lambda\bar{\rho}_\uparrow\mathbf{k}\cdot\mathbf{k}'\right]\bar{\psi}_{\uparrow\mathbf{k}}\bar{\psi}_{\downarrow\mathbf{k}'+\mathbf{q}}\psi_{\downarrow\mathbf{k}+\mathbf{q}}\psi_{\uparrow\mathbf{k}'}+\int\mathrm{d}\mathbf{k}'\mathrm{d}\mathbf{q}\left[g+\mathrm{i}\lambda\bar{\rho}_\downarrow\mathbf{k}\cdot\mathbf{k}'\right]\bar{\psi}_{\uparrow\mathbf{k}+\mathbf{q}}\bar{\psi}_{\downarrow\mathbf{k}'}\psi_{\downarrow\mathbf{k}}\psi_{\uparrow\mathbf{k}'+\mathbf{q}}\Bigg]. \tag{4}$$

Finally we focus on the momentum dependence of the two-body term. In Ref. [5] it was shown that the dominant contribution due to fluctuation contributions stemmed from electron-hole excitations at the Fermi surface near to $|\mathbf{k}+\mathbf{k}'| = 2k_\mathrm{F}$, and therefore the principal contribution to the action from fluctuation corrections stems from $\mathbf{k}\cdot\mathbf{k}' = -k_\mathrm{F}^2$. Using this we recover the action

$$S=\int_0^\beta\mathrm{d}\tau\mathrm{d}\mathbf{k}\Bigg[\sum_\sigma\bar{\psi}_{\sigma\mathbf{k}}\left(\partial_\tau+\epsilon_\mathbf{k}+\mathrm{i}\lambda\bar{\rho}_\uparrow\bar{\rho}_\downarrow k^2-\mu-\mathrm{i}\gamma\right)\psi_{\sigma\mathbf{k}}+\int\mathrm{d}\mathbf{k}'\mathrm{d}\mathbf{q}\left[g-\mathrm{i}\lambda(\bar{\rho}_\uparrow\mu_\uparrow+\bar{\rho}_\downarrow\mu_\downarrow)\right]\bar{\psi}_{\uparrow\mathbf{k}+\mathbf{q}}\bar{\psi}_{\downarrow\mathbf{k}'}\psi_{\downarrow\mathbf{k}}\psi_{\uparrow\mathbf{k}'+\mathbf{q}}\Bigg], \tag{5}$$

where the Fermi surface of the separate spin species is $\mu_\sigma = k_{\mathrm{F},\sigma}^2/2$.

To proceed we calculate the free energy following the prescription laid out in Ref. [9]. First we introduce a Hubbard-Stratonovich transformation in both the density channel ρ and the magnetization channel $\boldsymbol{\phi}$ to decouple the quartic terms in the fermionic field. This leads us to identify the spectrum $\xi_{\mathbf{k},\sigma} = \epsilon_\mathbf{k} + \mathrm{i}\lambda\bar{\rho}_\uparrow\bar{\rho}_\downarrow k^2/2 - \mathrm{i}\gamma + [g - \mathrm{i}\lambda(\bar{\rho}_\uparrow\mu_\uparrow + \bar{\rho}_\downarrow\mu_\downarrow)](\rho - \sigma\phi) - \mu$. After integrating out the fermionic variables we expand the fluctuations in the bosonic fields to quadratic order and also integrate them out. To remove the unphysical ultraviolet divergence of the contact interaction we employ the standard regularization setting $g \mapsto \frac{2k_\mathrm{F}a}{\pi\nu} - \frac{2}{V}(\frac{2k_\mathrm{F}a}{\pi\nu})^2\sum'_{\mathbf{k}_{3,4}}(\xi_{\mathbf{k}_1,\uparrow} + \xi_{\mathbf{k}_2,\downarrow} - \xi_{\mathbf{k}_3,\uparrow} - \xi_{\mathbf{k}_4,\downarrow})^{-1}$ [19]. The prime indicates that the summation is subject to the momentum conservation $\mathbf{k}_1 + \mathbf{k}_2 = \mathbf{k}_3 + \mathbf{k}_4$ and ν is the density of states at the Fermi surface of an equivalent non-interacting gas. This regularization allows us to characterize the strength of the interaction through the dimensionless parameter $k_\mathrm{F}a$, where k_F denotes the Fermi wave vector and a is the s-wave scattering length. The analysis yields a perturbation expansion in terms of the dimensionless interaction strength $k_\mathrm{F}a$ and the loss parameter λ. We now set the fields to their as yet undetermined saddle point values $\rho = (\bar{\rho}_\uparrow + \bar{\rho}_\downarrow)/2$ and $\phi = (\bar{\rho}_\uparrow - \bar{\rho}_\downarrow)/2$ to yield the complex free energy

$$\begin{aligned}\mathcal{F} = &\sum_\sigma\int\mathrm{d}\mathbf{k}(\epsilon_\mathbf{k} + \mathrm{i}\lambda\bar{\rho}_\uparrow\bar{\rho}_\downarrow k^2/2 - \mathrm{i}\gamma)n(\xi_{\mathbf{k},\sigma})\\ &+\left[\frac{2k_\mathrm{F}a}{\pi\nu} - \mathrm{i}\lambda(\bar{\rho}_\uparrow\mu_\uparrow + \bar{\rho}_\downarrow\mu_\downarrow)\right]\sum_\mathbf{k}n(\xi_{\mathbf{k},\uparrow})\sum_\mathbf{k}n(\xi_{\mathbf{k},\downarrow})\\ &-2\left[\frac{2k_\mathrm{F}a}{\pi\nu} - \mathrm{i}\lambda(\bar{\rho}_\uparrow\mu_\uparrow + \bar{\rho}_\downarrow\mu_\downarrow)\right]^2\Upsilon\,,\end{aligned} \tag{6}$$

where the quantum fluctuations are encoded in the term

$$\Upsilon = {\sum_{\mathbf{k}_{1,2,3,4}}}'\frac{n(\xi_{\mathbf{k}_1,\uparrow})n(\xi_{\mathbf{k}_2,\downarrow})\left[n(\xi_{\mathbf{k}_3,\uparrow}) + n(\xi_{\mathbf{k}_3,\downarrow})\right]}{\xi_{\mathbf{k}_1,\uparrow} + \xi_{\mathbf{k}_2,\downarrow} - \xi_{\mathbf{k}_3,\uparrow} - \xi_{\mathbf{k}_4,\downarrow}}\,, \tag{7}$$

and now $\xi_{\mathbf{k},\sigma} = \epsilon_\mathbf{k} + \mathrm{i}\lambda\bar{\rho}_\uparrow\bar{\rho}_\downarrow k^2/2 - \mathrm{i}\gamma + [2k_\mathrm{F}a/\pi\nu - \mathrm{i}\lambda(\bar{\rho}_\uparrow\mu_\uparrow + \bar{\rho}_\downarrow\mu_\downarrow)]\bar{\rho}_\sigma - \mu$.

To analyze this complex free energy $\mathcal{F}$, we shall separate it into its real and imaginary parts. In Sec. IV we will study the phase diagram inferred from considering only the real part of the free energy. The imaginary part betrays the fact the system is not in true equilibrium.

Constant loss of particles leads to slow heating and depletion of the system, whose effects cannot be studied within our imaginary time formalism. In section Sec. VI we shall use kinetic equations to show that the net effect of these terms is to drive an effective equilibrium state with slowly rising temperature.

To facilitate the splitting of the free energy, we now separate the spectrum $\xi_{\mathbf{k},\sigma} = \xi^0_{\mathbf{k},\sigma} + \mathrm{i}\Delta_{\mathbf{k},\sigma}$ into its real part $\xi^0_{\mathbf{k},\sigma} = \epsilon_{\mathbf{k}} + 2k_{\mathrm{F}}a\bar{\rho}_\sigma/\pi\nu - \mu$ and imaginary part $\Delta_{\mathbf{k},\sigma} = \lambda\bar{\rho}_\uparrow\bar{\rho}_\downarrow k^2/2 - \gamma - \lambda(\bar{\rho}_\uparrow\mu_\uparrow + \bar{\rho}_\downarrow\mu_\downarrow)\bar{\rho}_\sigma$. We notice that the imaginary part $\Delta_{\mathbf{k},\sigma}$ is perturbatively small in λ and γ. Consistent with the perturbation expansion in the interaction strength, we use the low temperature expression $n(\xi^0_{\mathbf{k},\sigma} + \mathrm{i}\Delta_{\mathbf{k},\sigma}) \approx n(\xi^0_{\mathbf{k},\sigma}) - \mathrm{i}\Delta_{\mathbf{k},\sigma}\delta(\xi^0_{\mathbf{k},\sigma}) + \Delta^2_{\mathbf{k},\sigma}\delta'(\xi^0_{\mathbf{k},\sigma})/2$ to expand the Fermi-Dirac distributions in Eq. (6) and Eq. (7) out to quadratic order in $\Delta_{\mathbf{k},\sigma}$. We see that contributions to the free energy that are quadratic in $\Delta_{\mathbf{k},\sigma}$ are real and so will contribute to the real part of the free energy whereas the linear order terms are imaginary.

The real part of the free energy is $F = F_0 + \Lambda(\lambda)$, where the standard theory of a lossless system is encoded in the term

$$F_0 = \sum_{\sigma,\mathbf{k}} \epsilon_{\mathbf{k}} n(\xi^0_{\mathbf{k},\sigma}) + \frac{2k_{\mathrm{F}}a}{\pi\nu}\bar{\rho}_\uparrow\bar{\rho}_\downarrow - 2\left(\frac{2k_{\mathrm{F}}a}{\pi\nu}\right)^2 \Upsilon_0 \,. \quad (8)$$

An identical expression was derived in the homogeneous case in Ref. [1, 4, 9] using second order perturbation theory. The renormalization of the interaction strength due to atom loss enters through

$$\begin{aligned}\Lambda = {} & 2\lambda^2(\bar{\rho}_\uparrow\mu_\uparrow + \bar{\rho}_\downarrow\mu_\downarrow)^2\left(\Upsilon_0 - \sum_\sigma \bar{\rho}^2_{-\sigma}\mu_\sigma\nu'_\sigma\right) \\ & + \lambda(\bar{\rho}_\uparrow\mu_\uparrow + \bar{\rho}_\downarrow\mu_\downarrow)\sum_\sigma(\gamma - \lambda\bar{\rho}_\uparrow\bar{\rho}_\downarrow\mu_\sigma)\bar{\rho}_{-\sigma}(\nu_\sigma - 2\mu_\sigma\nu'_\sigma) \\ & + \sum_\sigma(\gamma - \lambda\bar{\rho}_\uparrow\bar{\rho}_\downarrow\mu_\sigma)^2\left[\frac{\nu_\sigma}{2} - \mu_\sigma\nu'_\sigma\right], \end{aligned} \quad (9)$$

where ν_σ denotes the density of states at the Fermi energy of species σ, and ν'_σ is the differential of the density of states at the Fermi surface. Only those terms containing

$$\Upsilon_0 = {\sum_{\mathbf{k}_{1,2,3,4}}}' \frac{n(\xi^0_{\mathbf{k}_1,\uparrow})n(\xi^0_{\mathbf{k}_2,\downarrow})\left[n(\xi^0_{\mathbf{k}_3,\uparrow}) + n(\xi^0_{\mathbf{k}_3,\downarrow})\right]}{\xi^0_{\mathbf{k}_1,\uparrow} + \xi^0_{\mathbf{k}_2,\downarrow} - \xi^0_{\mathbf{k}_3,\uparrow} - \xi^0_{\mathbf{k}_4,\downarrow}}, \quad (10)$$

are embedded with quantum many-body effects realized through fluctuation corrections. The remainder are mean-field terms derived from expanding the kinetic energy and Stoner interaction terms.

We now turn to obtain the imaginary part of the free energy. This is

$$\begin{aligned} & \lambda\left(\bar{\rho}_\uparrow\bar{\rho}_\downarrow\sum_\sigma\mu^2_\sigma\nu_\sigma - \sum_\sigma\bar{\rho}_\sigma\mu_\sigma\sum_{\sigma'}\bar{\rho}_{\sigma'}\mu_{-\sigma'}\nu_{-\sigma'}\right) \\ & - \gamma\left(\sum_\sigma\bar{\rho}_\sigma + \mu_\sigma\nu_\sigma\right). \end{aligned} \quad (11)$$

The actual experiment is most naturally described by setting $\gamma = 0$, and in this case we have an imaginary term in the free energy that drives actual loss from the system. We shall complement the $\gamma = 0$ approach with one that compensates for the three-body loss with a linear gain term $\gamma > 0$. Strictly speaking, the phase boundary is defined only in this case which describes a steady state. Having no net loss demands that there is no imaginary component to the free energy, which fixes the atom source term to

$$\gamma_{\mathrm{eq}} = \lambda\frac{\sum_\sigma\bar{\rho}_\sigma\mu_\sigma\sum_{\sigma'}\bar{\rho}_{\sigma'}\mu_{-\sigma'}\nu_{-\sigma'} - \bar{\rho}_\uparrow\bar{\rho}_\downarrow\sum_\sigma\mu^2_\sigma\nu_\sigma}{\sum_\sigma\bar{\rho}_\sigma + \mu_\sigma\nu_\sigma}. \quad (12)$$

Here ν_σ denotes the density of states at the Fermi energy of species σ. We note that the atom loss is zero when the system is fully polarized and then in any case $\gamma = 0$.

IV. PHASE DIAGRAM

Having derived an expression for the free energy we now turn to study its phase diagram. To determine the phase diagram we use the real part of the free energy, focusing on the boundary of the fully polarized state. Later, in Sec. VI we will return to address the loss dynamics implied by the imaginary part of the free energy and determine in which situations it can be safely neglected.

We first consider the mean-field approximation obtained by neglecting the fluctuation corrections Υ_0 in the free energy. As seen in Fig. 2(a,c), within the mean-field approximation atom loss stabilizes the fully polarized phase, which consequentially can be seen at weaker interaction strengths, and the transition remains second order. When we consider the collective modes in Sec. V we will see that there is a maximum loss rate $\lambda = 2^{5/3}3/5\pi\nu$ beyond which the fully polarized state cannot be formed, bounding the fully polarized region.

When fluctuations are taken into account in Fig. 2(b,d), we see two important changes. First, without loss ($\lambda = 0$) the fluctuations reduce the critical interaction strength needed to enter the ferromagnetic phase ($k_{\mathrm{F}}a \approx 1.05$) as compared to the mean-field theory ($k_{\mathrm{F}}a^* = 2^{5/3}3/5 \approx 1.9$), and also drive the transition to be first order. This has been pointed out before in Refs. [4, 5, 9]. Second, with loss, the interaction strength required to enter the ferromagnetic phase increases. Moreover, for sufficiently high loss the transition reverts from being first order back to second order. These are consequences of the dissipative effect of loss on the quantum fluctuations, which can be exposed by returning to Eq. (8) and Eq. (9), and noting that the total contribution to the free energy from the quantum fluctuations, that is all terms proportional to Υ_0, is $2\Upsilon_0[\lambda^2(\bar{\rho}_\uparrow\mu_\uparrow + \bar{\rho}_\downarrow\mu_\downarrow)^2 - (2k_{\mathrm{F}}a/\pi\nu)^2]$. We see that increasing loss acts in opposition to increasing interaction strength so loss removes the first order transition and

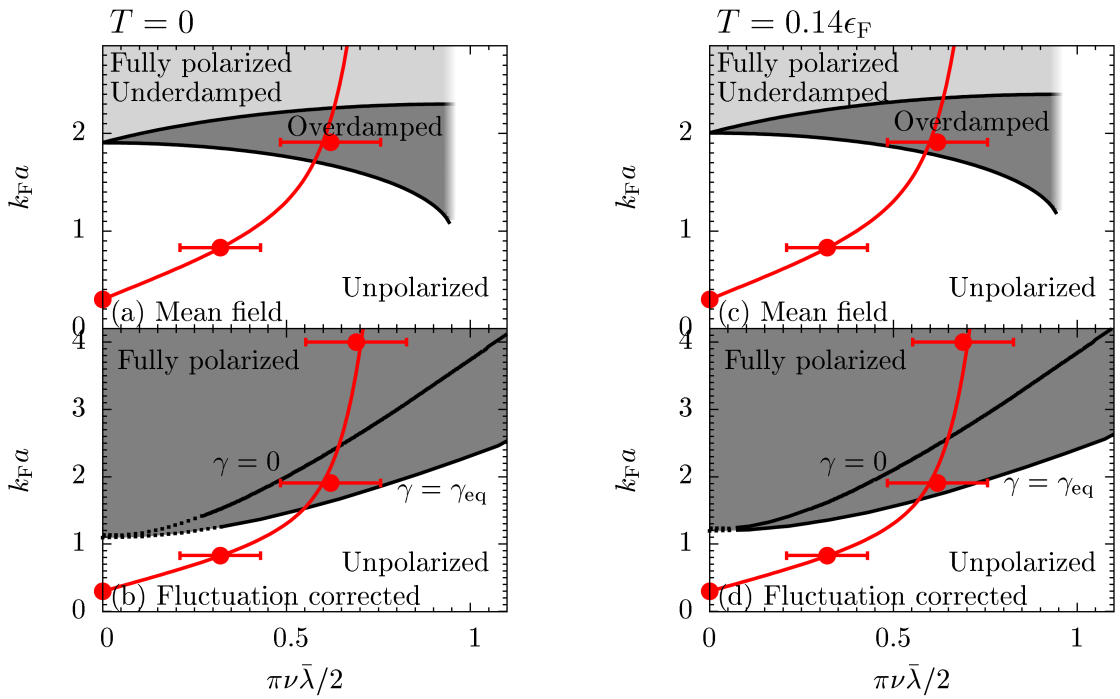

FIG. 2: (Color online) The required interaction strength at (left) $T = 0$ and (right) $T = 0.14\epsilon_{\rm F}$ to reach the shaded full polarization with changing loss rate λ in (a,c) the mean-field case and (b,d) when fluctuation corrections are considered. The experimental [20] atom loss variation is shown by the red points and accompanying trajectory. In (a,c) the regions where collective modes are underdamped and overdamped are highlighted, and the ferromagnetic transition is always second order. The ferromagnetic state is not stable beyond $\lambda = 2^{5/3}3/5\pi\nu$ (see Sec. V). In (b,d) the phase boundary is shown in the absence of atom source ($\gamma = 0$) and with an atom source that compensates for loss ($\gamma = \gamma_{\rm eq}$). The first order fully polarized boundary is plotted with the dotted line, and the second order boundary is shown by the solid line.

raises the interaction strength that the transition is seen at.

Having understood the main features of the phase diagram in the presence of loss we now focus on how it varies when we consider two additional parameters: an atom source and temperature. In the presence of an atom source that compensates the loss ($\gamma = \gamma_{\rm eq}$) the system displays the same qualitative behavior, though the transition takes place at a reduced interaction strength. All the effects are in essence unchanged by the compensating source term, because they stem from an inherently quantum mechanism underlying the renormalization of the interaction strength, rather than a purely classical fall in the atom number. The consistency of the predicted boundaries for $\gamma = 0$ and $\gamma = \gamma_{\rm eq}$ also verifies the robustness of our approach. Secondly, we will show in Sec. VI that loss blurs the Fermi surface so raises the effective temperature of the system. We focus on the special temperature $0.14\epsilon_{\rm F}$, which we show in Sec. VI corresponds to the loss driven temperature rise for the particular experimental parameters. Finite temperature has only a small effect on the phase diagram, and chiefly reduces the range over which the transition is first order rather than second order. This is because we are approaching the tricritical point at $T \approx 0.2\epsilon_{\rm F}$ [4], where the transition reverts to being second order even in the absence of loss.

V. EXPERIMENTAL OBSERVATION

Having studied the phase diagram Fig. 2, we now turn to consider how it could be probed experimentally, and the impact of loss on properties of the ferromagnetic phase. In the strongly interacting regime we use experimental results [20] to determine how the loss rate varies with interaction strength, and interpolate the trajectory that the atom gas follows through the phase diagram. The system undergoes a second order transition into the fully polarized phase at $k_{\rm F}a \approx 2.4$, which compares favorably with the experimental observation that the atomic gas became fully polarized at $k_{\rm F}a \approx 2.2$ [10]. The observation of a significantly raised critical interaction strength, compared to the equilibrium theory ($k_{\rm F}a \approx 1.0$) [6, 11], is therefore strongly suggestive of the important role that the damping of quantum fluctuations has to play.

Collective modes in the ferromagnet. We now consider the impact of loss on the collective spin excitations of the ferromagnet. We focus on the fully polarized regime,

where we have only transverse collective modes driven by the inverse propagator $1+\frac{2k_{\rm F}a}{\pi\nu}\sum_{\omega,\mathbf{p}}G_{\uparrow}(\omega+\Omega,\mathbf{p}+\mathbf{q})G_{\downarrow}(\omega,\mathbf{p})$ [9]. Equating this to zero yields collective mode frequencies with both a real and an imaginary part. The real part, which gives the collective mode dispersion is

$$\Omega=\frac{q^2}{2}\left(1-\frac{k_{\rm F}a^*}{k_{\rm F}a}\frac{1}{1+\tilde{\lambda}^2/(k_{\rm F}a)^2}\right), \tag{13}$$

where $\tilde{\lambda}=\lambda(\bar{\rho}_{\uparrow}\mu_{\uparrow}+\bar{\rho}_{\downarrow}\mu_{\downarrow})$ and $k_{\rm F}a^*=2^{5/3}3/5$ denotes the interaction strength of the mean-field Stoner instability to full polarization. Disregarding losses, the collective modes dispersion is identical to that found by Callaway [21]. The quadratic spin dispersion is equal to that of a single minority spin species particle propagating through a sea of majority spin particles. The dispersion rises with increasing interaction strength $k_{\rm F}a$ as the system becomes stiffer against spin rotation. Atom loss introduces an additional energy penalty for fluctuations, and consequentially the dispersion also rises with the loss rate parameter $\tilde{\lambda}$. To fully expose the influence that atom loss has over the dispersion it is useful to focus on the instability to a partially polarized phase which develops at

$$k_{\rm F}a=\frac{k_{\rm F}a^*}{2}+\sqrt{\frac{(k_{\rm F}a^*)^2}{4}-\tilde{\lambda}^2}\,. \tag{14}$$

Without three-body loss, the fully polarized phase becomes unstable at $k_{\rm F}a=k_{\rm F}a^*$ in accordance with the prediction of the mean-field Stoner model. At mean-field level fluctuations destroy the ferromagnetic state, so Eq. (14) matches the boundary Fig. 2(a,c) which demonstrates how increased loss reduces the required interaction strength. Working at the mean-field level, there is a maximum loss rate, $\tilde{\lambda}=k_{\rm F}a^*/2$, beyond which the fully polarized state cannot be formed.

In addition to renormalizing the dispersion, the presence of a loss interaction also leads to the decay of the spin excitations. As the spin wave propagates the atom spins develop a component in the opposite spin direction and so incurs atom loss, which in turn damps the spin wave. The characteristic inverse timescale of damping, or width, of a transverse mode can be found from the imaginary component of its frequency,

$$\Gamma=\frac{q^2}{2}\frac{k_{\rm F}a^*\tilde{\lambda}}{(k_{\rm F}a)^2}\frac{1}{1+\tilde{\lambda}^2/(k_{\rm F}a)^2}\,. \tag{15}$$

We see that due to atom loss the spin-waves become resonances that are characterized by a momentum independent quality factor

$$Q\equiv\frac{\Omega}{\Gamma}=\frac{1}{k_{\rm F}a^*}\left(\frac{(k_{\rm F}a)^2}{\tilde{\lambda}}+\tilde{\lambda}\right)-\frac{k_{\rm F}a}{\tilde{\lambda}}\,. \tag{16}$$

In Fig. 2(a,c) we highlight the region $Q<1$, where spin excitations completely lose their integrity.

In experiment, these collective modes can be excited and probed by spin-dependent Bragg spectroscopy. A variable wavelength optical lattice potential couples asymmetrically to the spin degrees of freedom, and thereby excites transverse magnetic fluctuations. The collective mode response could be studied through dynamical fluctuations of the cloud spatial distribution as a function of wavelength, laser amplitude, and detuning.

An experimental handle that could modify the atom loss rate would gift investigators with the ability to fully explore the consequences of atom loss. This can be achieved for example using an additional bosonic [22] or different fermion [23] species that would act as a third body. The loss rate will be proportional to the density of this third species, which can be conveniently controlled.

VI. LOSS DRIVEN HEATING & QUASIEQUILIBRIUM CRITERION

In the previous sections we studied the phase diagram by considering the real part of the free energy Eq. (11), while neglecting the imaginary part. This is based on an assumption that at each instant the system can be described by an effective equilibrium. In this section we shall study the validity of this assumption.

Besides causing a net decrease in particle number, loss events also tend to drive the system out of equilibrium by producing "holes" in the Fermi distribution. At the same time, two-particle collisions act to relax the distribution and restore equilibrium. We shall use the Boltzmann kinetic equation to study the interplay of these effects. We will show that the time dependent distribution function is just the equilibrium Fermi-Dirac distribution, but with a temperature that is slowly increasing with time and a decreasing chemical potential. In the next stage we check under what conditions the time dependence thus induced is sufficiently slow as not to mask the interesting fluctuation effects found in the previous sections.

The kinetic equation for the lossy Fermi liquid is given by

$$\frac{{\rm d}n_{\mathbf{k},\sigma}}{{\rm d}t}=\left(\frac{\partial n_{\mathbf{k},\sigma}}{\partial t}\right)_{\rm coll}+\left(\frac{\partial n_{\mathbf{k},\sigma}}{\partial t}\right)_{\rm loss}. \tag{17}$$

The terms on the right-hand side acting on the distribution function $n_{\mathbf{k},\sigma}$ correspond to the relaxation rate of atoms and the three-body loss. In the steady state the collisional relaxation rate is

$$\left(\frac{\partial n_{\mathbf{k},\sigma}}{\partial t}\right)_{\rm coll}=-\frac{n_{\mathbf{k},\sigma}}{\tau^{\rm e}_{\mathbf{k}}}+\frac{1-n_{\mathbf{k},\sigma}}{\tau^{\rm h}_{\mathbf{k}}}\,, \tag{18}$$

where the inverse lifetime of the quasiparticles is $1/\tau^{\rm e}_{\mathbf{k}}=4(\epsilon-\epsilon_{\rm F})^2(k_{\rm F}a)^2(1-N^{\rm eq}_{\mathbf{k},\sigma})/\hbar\epsilon_{\rm F}$ and quasiholes is $1/\tau^{\rm h}_{\mathbf{k}}=4(\epsilon-\epsilon_{\rm F})^2(k_{\rm F}a)^2N^{\rm eq}_{\mathbf{k},\sigma}/\hbar\epsilon_{\rm F}$, with the thermal equilibrium Fermi-Dirac distribution $N^{\rm eq}_{\mathbf{k},\sigma}$. Combined these give the

net collisional relaxation rate

$$\left(\frac{\partial n_{\mathbf{k},\sigma}}{\partial t}\right)_{\rm coll} = \frac{4(\epsilon-\epsilon_{\rm F})^2(k_{\rm F}a)^2}{\hbar\epsilon_{\rm F}}\left(N^{\rm eq}_{\mathbf{k},\sigma}-n_{\mathbf{k},\sigma}\right). \quad (19)$$

Having setup the relaxation process that aims to restore the equilibrium Fermi distribution we now turn to the three-body loss process that causes particles to be removed. In the weak coupling regime $k_{\rm F}a \ll 1$ loss occurs at a rate of [14]

$$\left(\frac{\partial n_{\mathbf{k},\sigma}}{\partial t}\right)_{\rm loss} = -2\Gamma_0(k_{\rm F}a)^6\bar{n}^2 n_{\mathbf{k},\sigma}\,, \quad (20)$$

where $\bar{n}=\sum_{\mathbf{k}} n_{\mathbf{k}}$ is the average density of one species of the particles. With the rate of the two dynamical processes established we are now in a position to write down the kinetic equation for the whole system

$$\frac{{\rm d}n_{\mathbf{k},\sigma}}{{\rm d}t} = \frac{4(\epsilon-\epsilon_{\rm F})^2(k_{\rm F}a)^2}{\hbar\epsilon_{\rm F}}\left(N^{\rm eq}_{\mathbf{k},\sigma}-n_{\mathbf{k},\sigma}\right) - 2\Gamma_0(k_{\rm F}a)^6\bar{n}^2 n_{\mathbf{k},\sigma}. \quad (21)$$

There are two time-scales in the system: the loss rate of atoms and the collisional relaxation rate. Fortunately they are typically well separated scales. At least at weak coupling, and apparently also in the experiment, the collisional relaxation rate is significantly quicker than the loss rate. Hence the collisional term forces the distribution $n_{\mathbf{k},\sigma}$ to be equal to the Fermi-Dirac distribution $N^{\rm eq}_{\mathbf{k},\sigma}$, albeit with time dependent parameters μ and T. If the system is perturbed from the Fermi-Dirac distribution such that $n_{\mathbf{k},\sigma}=N^{\rm eq}_{\mathbf{k},\sigma}+\eta_{\mathbf{k},\sigma}$, then that perturbation decays exponentially with time with the usual decay rate of a Fermi liquid quasi-particle $\tau^{-1}\propto(k_{\rm F}a)^2(\epsilon-\epsilon_{\rm F})^2/\epsilon_{\rm F}$.

The time dependence of the chemical potential and the temperature can be found from the equation ${\rm d}n_{\mathbf{k},\sigma}/{\rm d}t = -2\Gamma_0(k_{\rm F}a)^6\bar{n}^2 n_{\mathbf{k},\sigma}$ obtained when we substitute the Fermi-Dirac ansatz for the distribution. If we sum over momenta we recover the integrated form

$$\frac{\partial\bar{n}}{\partial\mu}\frac{{\rm d}\mu}{{\rm d}t}+\frac{\partial\bar{n}}{\partial T}\frac{{\rm d}T}{{\rm d}t} = -\Gamma_0(k_{\rm F}a)^6\bar{n}^3\,. \quad (22)$$

At low temperature, the term ${\rm d}\bar{n}/{\rm d}T \propto T$ can be neglected. We can then solve the remaining equation to find that the chemical potential falls as $\mu = \mu_0/\sqrt[3]{1+4\Gamma_0(k_{\rm F}a)^6\bar{n}^2 t}$. Now, to obtain the time dependent temperature we return to the kinetic equation, multiply by the kinetic energy, and again sum over momenta to get

$$\frac{\partial\bar{E}}{\partial\mu}\frac{{\rm d}\mu}{{\rm d}t}+\frac{\partial\bar{E}}{\partial T}\frac{{\rm d}T}{{\rm d}t} = -\Gamma_0(k_{\rm F}a)^6\bar{n}^2\bar{E}\,, \quad (23)$$

where $\bar{E}=\sum_{\mathbf{k},\sigma}\epsilon_{\mathbf{k},\sigma}n_{\mathbf{k}}$. Substituting in our solution for the chemical potential, we find that temperature rises as

$$T = \sqrt{T_0^2-\frac{2\mu_0^2}{15\pi^2k_{\rm B}^2}\left[(1+4\Gamma_0(k_{\rm F}a)^6\bar{n}^2t)^{-2/3}-1\right]}\,. \quad (24)$$

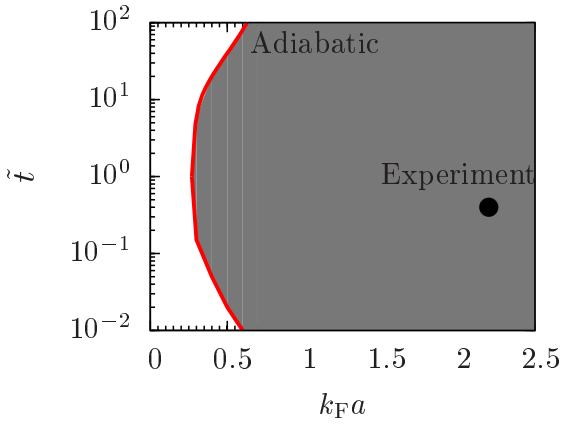

FIG. 3: Satisfaction of the adiabaticity criterion. The shaded area marks the region in the space of interaction strength and time in which the adiabacity criterion is satisfied if the system starts the evolution at $T=T_0=0$. The experimental parameters where ferromagnetism is first expected is highlighted by the black point.

In the long time limit, for the relevant experimental parameters, we find a predicted rise in the effective temperature of $\sim 0.14\epsilon_{\rm F}$ and fall in chemical potential to $\mu = 0.92\mu_0$. By comparing Fig. 2(a,b) at $T=0$ to Fig. 2(c,d) at $T=0.14\epsilon_{\rm F}$ we can see that the rise in effective temperature only slightly renormalizes the phase boundaries. However, in the vicinity of the tricritical point, where the transition reverts from first to second order, loss can turn the Stoner transition second order just due to heating, even without the quantum effects of the three-body loss. The fall in chemical potential results in a negligible reduction in the interaction strength to $0.97k_{\rm F}a$ and only a small impact on the observed phase boundaries. The main effect of loss is the damping of quantum fluctuations treated in the previous sections.

Having understood the consequences of the loss driven heating of the system we now turn to check if the system can be considered to be quasistatic. Specifically we would like to check if the time dependence is indeed slow compared to the loss induced corrections to the free energy (9) that lead to the phase diagrams shown in Fig. 2. Adiabaticity then requires that $\frac{1}{T}\frac{{\rm d}T}{{\rm d}\tilde{t}}<\Lambda$. It is helpful to turn to a dimensionless timescale, $\tilde{t}=4\Gamma_0(k_{\rm F}a)^6\bar{n}^2t$ and temperature $\tilde{T}=T\sqrt{15\pi^2k_{\rm B}^2/2\mu_0^2}$, and to define $\chi = 2(\bar{\rho}_\uparrow\mu_\uparrow+\bar{\rho}_\downarrow\mu_\downarrow)^2(\Upsilon_0-\sum_\sigma\bar{\rho}_{-\sigma}^2\mu_\sigma\nu'_\sigma)/(\bar{\rho}_\uparrow\bar{\rho}_\downarrow\sum_\sigma\mu_\sigma^2\nu_\sigma - \sum_\sigma\bar{\rho}_\sigma\mu_\sigma\sum_{\sigma'}\bar{\rho}_{\sigma'}\mu_{-\sigma'}\nu_{-\sigma'})^2$. The adiabaticity condition then translates to

$$\frac{(1+\tilde{t})^{3/2}}{3\sqrt{\tilde{T}_0^2+1-(1+\tilde{t})^{-2/3}}} < \chi(k_{\rm F}a)^6\,. \quad (25)$$

We show the set of parameters that satisfy adiabacity in Fig. 3. The criterion is not satisfied at weak interactions $k_{\rm F}a \ll 1$ because even here the temperature rises at a finite rate, while it is satisfied over an increasing time window at interaction strengths $k_{\rm F}a \gtrsim 0.3$. We note

that at the phase boundary the $(k_{\rm F}a)^6$ loss law used in this analysis still holds, and we have also verified that the adiabaticity criterion still applies at $k_{\rm F}a = 2.3$ with the experimentally determined loss rate [20]. Therefore, our formalism is expected to capture the consequences of damping on the ferromagnetic transition.

VII. CONCLUSIONS AND OUTLOOK

In this paper we considered the problem of three-body loss, inherent to a Fermi gas with effective repulsive interactions. We argued, using kinetic equations, that in a large parameter regime the lossy Fermi liquid can be treated as an effective-equilibrium system. In this case the quantum effects of loss can be derived within a simple imaginary time formalism. We have shown that these quantum effects can have a significant impact on the nature of the ferromagnetic transition. Loss damps quantum-fluctuations and thereby leads to an increase in the critical interaction strength to a value consistent with the experimental findings. Furthermore, in presence of loss the transition reverts from being first to second order. We have highlighted signatures of this mechanism in the collective mode spectrum.

More generally, we have shown that upon integrating out the collision products, the loss interaction gives rise to imaginary coupling terms in the effective action, in addition to the repulsive contact interactions. These terms could have an interesting impact on the nature of the Fermi liquid in this regime. An intriguing question for future investigation is how the presence of small loss affects the elementary excitations of the Fermi liquid? Are new modes or instabilities generated in presence of the new terms? Finally, the novel phenomenology that has been developed here opens the possibility to explore how loss affects other systems. The formalism could be directly applied to a wide range of problems across condensed matter physics. A particularly topical example where our formalism may well make a useful contribution are polariton condensates [24]. These systems are inherently out of equilibrium due to the finite lifetime of the polaritons which is typically treated as a two-body loss term. Our analysis may also shed light on the consequences of the strong loss in p-wave fermion superfluids and the pairing transition in a superfluid Bose gas [25].

VIII. ACKNOWLEDGEMENTS

We thank Eugene Demler, Andrew Green, Ben Simons, Dimitry Feldman, Ari Turner, Gyu-Boong Jo, Wolfgang Ketterle, and Joseph Thywissen for useful discussions. This research was supported in part by the National Science Foundation under Grant No. NSF PHY05-51164. GJC acknowledges the financial support of the Royal Commission for the Exhibition of 1851 and the Kreitman Foundation EA was supported in part by ISF under grant 910/07, and by the US-Israel BSF.

* Electronic address: gjc29@cam.ac.uk

[1] A.A. Abrikosov and I.M. Khalatnikov, Soviet Phys. JETP **6**, 888 (1958); F. Mohling, Phys. Rev. **122**, 1062 (1961).
[2] D. Belitz *et al.*, Phys. Rev. B **58**, 14155 (1998). M. Shimizu. Proc. Phys. Soc. **84**, 397 (1964); D. Belitz, T.R. Kirkpatrick, and T. Vojta. Phys. Rev. B **55**, 9452 (1997); J. Betouras, D. Efremov and A. Chubukov. Phys. Rev. B **72**, 115112 (2005); D.V. Efremov, J.J. Betouras and A. Chubukov. Phys. Rev. B **77**, 220401(R) (2008).
[3] M. Houbiers *et al.*, Phys. Rev. A **56**, 4864 (1997); L. Salasnich *et al.*, J. Phys. B: At. Mol. Opt. Phys. **33**, 3943 (2000); M. Amoruso *et al.*, Eur. Phys. J. D **8**, 361 (2000); T. Sogo and H. Yabu, Phys. Rev. A **66**, 043611 (2002).
[4] R.A. Duine and A.H. MacDonald, Phys. Rev. Lett. **95**, 230403 (2005).
[5] G.J. Conduit, A.G Green and B.D. Simons. Phys. Rev. Lett. **103**, 207201 (2009).
[6] L.J. LeBlanc *et al.*, Phys. Rev. A **80**, 013607 (2009).
[7] R. Borzi *et al.*, Science **315**, 214 (2007); M. Uhlarz, C. Pfleiderer and S.M. Hayden, Phys. Rev. Lett. **93**, 256404 (2004).
[8] I. Berdnikov, P. Coleman and S.H. Simon. Phys. Rev. B **79**, 224403 (2009).
[9] G.J. Conduit and B.D. Simons. Phys. Rev. A **79**, 053606 (2009).
[10] G.-B. Jo *et al.*, Science **325**, 1521 (2009).
[11] G.J. Conduit and B.D. Simons. Phys. Rev. Lett. **103**, 200403 (2009).
[12] M. Babadi *et al.*, arXiv:0908.3483 (2009).
[13] H. Zhai, Phys. Rev. A **80**, 051605(R) (2009).
[14] D.S. Petrov. Phys. Rev. A **67**, 010703(R) (2003).
[15] N. Syassen *et al.*, Science **320**, 1329 (2009); S. Durr *et al.*, Phys. Rev. A **79**, 023614 (2009); A.J. Daley *et al.*, Phys. Rev. Lett. **102**, 040402 (2009).
[16] S. Pilati, G. Bertaina, S. Giorgini and M. Troyer, Phys. Rev. Lett. **105**, 030405 (2010).
[17] S.-Y. Chang, M. Randeria, N. Trivedi, Proc. Natl. Acad. Sci. 108:51 (2011).
[18] R. Shankar, Rev. Mod. Phys. **66**, 129 (1994).
[19] R.K. Pathria, Statistical Mechanics, Pergamon Press (1996).
[20] J.H. Huckans *et al.*, Phys. Rev. Lett. **102**, 165302 (2009).
[21] J. Callaway, Phys. Rev. **170**, 576 (1968).
[22] J.J. Zirbel, K.-K. Ni, S. Ospelkaus, J.P. DIncao, C.E. Wieman, J. Ye and D.S. Jin, Phys. Rev. Lett. **100**, 143201 (2008); J.P. DIncao and B.D. Esry, Phys. Rev. A **73**, 030702(R) (2006); J.P. DIncao and B.D. Esry, Phys. Rev. Lett. **94**, 213201 (2005).
[23] A.N. Wenz *et al.*, Phys. Rev. A **80**, 040702(R) (2009).
[24] J. Kasprzak *et al.*, Nature **443**, 409 (2006)
[25] L. Radzihovsky, J. Park, and P.B. Weichman, Phys. Rev. Lett. **92**, 160402 (2004)